Suarez-Martinez, Pilar C.; Batys, Piotr; Sammalkorpi, Maria; Lutkenhaus, Jodie L.

Time-Temperature and Time-Water Superposition Principles Applied to Poly(allylamine)/Poly(acrylic acid) Complexes

Published in:
Macromolecules

DOI:
10.1021/acs.macromol.8b02512

Published: 23/04/2019

Document Version
Peer-reviewed accepted author manuscript, also known as Final accepted manuscript or Post-print

Time-Temperature and Time-Water Superposition Principles Applied to Poly(allylamine) / Poly(acrylic acid) Complexes

Pilar C. Suarez-Martinez[a], *Piotr Batys*[b,c,†], *Maria Sammalkorpi*[b] *and Jodie L. Lutkenhaus*[a,*]

[a]Artie McFerrin Department of Chemical Engineering, Texas A&M University, College Station, Texas 77843, United States

[b]Department of Chemistry and Materials Science, [c]Department of Bioproducts and Biosystems, School of Chemical Engineering, Aalto University, P.O. Box 16100, FI-00076 Aalto, Finland

[†]Jerzy Haber Institute of Catalysis and Surface Chemistry, Polish Academy of Sciences, Niezapominajek 8, PL-30239 Krakow, Poland

[*]Corresponding author

E-mail address: jodie.lutkenhaus@tamu.edu

Time, temperature, water content, relative humidity, superposition, polyelectrolyte complex, dynamic mechanical behavior

ABSTRACT

The dynamic mechanical and rheological behavior of polyelectrolyte coacervates and complex precipitates is of interest for many applications ranging from health to personal care. Hydration is an important factor, but its effect on the dynamic properties of polyelectrolyte complexes (PECs) is poorly understood. Here, we describe the dynamic behavior of poly(allylamine hydrochloride) (PAH) and poly(acrylic acid) (PAA) complex precipitates at varying relative humidity values and temperatures using both dynamic mechanical analysis (DMA) and all-atom molecular dynamics simulations. To mirror the experimental system via simulation, the water content within the PEC is measured and used as the parameter of interest, rather than relative humidity. In experimental DMA, modulus decreases with both increasing water content and temperature. The data are superimposed into a super-master hydrothermal curve using the time-temperature superposition principle and the time-water superposition principle for the first time. The temperature-dependent shift factor (a_T) follows an Arrhenius relation, and the water-dependent shift factor (a_w) follows a log-linear relation with water content in the complex. These results suggest that both temperature and water affect the dynamics of the PEC by similar mechanisms over the range investigated. All-atom molecular dynamics simulations show that an increase in water content and temperature lead to similar changes in polyelectrolyte chain mobility with little effect on the number of intrinsic ion pairs, suggesting the validity of time-water and time-temperature supposition principles.

INTRODUCTION

Polyelectrolyte complexes (PECs) are the product of strong interactions between oppositely charged macromolecules and the release of entropic counterions in solution.[1-22] PEC morphologies range from solid-like (polyelectrolyte complexes) to liquid-like (polyelectrolyte coacervates),[23, 24] and are affected by assembly conditions (*e.g.,* polyelectrolyte concentration, ionic strength and salt

type, polyelectrolyte type and molecular weight, *etc*.), as well as post-treatment conditions.[25-27] Consequently, PEC physical properties have proven to be affected by water content, salt, and pH.[28-42] This enables PECs for several applications including humidity sensors,[43, 44] adhesives,[45] self-healing materials,[46-49] and mechanically adaptive materials.[50] To date, it is generally accepted that water content and temperature affect the mechanical properties of PECs.[28-34] However, there is little information regarding the dynamic mechanical behavior of PECs as a function of both water content and temperature. A fundamental understanding is needed to not only reveal how polyelectrolyte chains behave dynamically within the complex but also for enabling certain applications.

PEC structure is generally described by intrinsic and extrinsic ion pairing. [23, 37] Intrinsic ion pairing is formed by the electrostatic interactions between oppositely charged polymer repeat units, and extrinsic ion pairing results from interactions of polymer repeat units and counter ions.[23] Water acts as an essential plasticizing agent, relaxing the polymer chains within the PEC. Increasing the water content in PECs causes an increase in free volume, structural rearrangement, and a decrease in both the PEC glass transition temperature and modulus.[25, 51] Salt facilitates PEC plasticization by transforming intrinsic ion pairs into extrinsic ion pairs, which promotes the relaxation of polyelectrolyte chains within the PEC. However, simulations indicate that the plasticizing effect of salt is influenced by water: salt acts as a plasticizer (weakening ion pairing) or a hardener (immobilizing the water molecules), depending on the PEC hydration level.[51] Thus, salt influences whether a hydrated PEC is glassy — moduli ~ 10^9 Pa — or rubbery — moduli ~ 10^6 Pa.[37, 52-54] Similarly, pH can have a strong effect on the number of intrinsic ion pairs by way of controlling a polyelectrolyte's charge density.[38, 55] Together, water, pH, and salt have been reported to influence static mechanical properties.[24, 25, 32, 37, 40, 51, 55]

Due to the known effects of water, salt, and pH on the structure and mechanical properties of PECs, the dynamic mechanical behavior of PECs has been studied through the application of superposition principles. Superposition principles are a tool used to study physical and mechanical responses of materials in the time domain (*e.g.,* polymers, polyelectrolyte complexes).[40, 56] Specifically, superposition principles are used to analyze frequency-dependent properties such as the complex modulus. The time-temperature superposition principle (TTSP), for example, relates the time and temperature response of viscoelastic materials.[56] Thus, TTSP is used to either determine the temperature-dependence of a material's rheological behavior, or to study a material's behavior at a specific temperature over a broader frequency range.[56, 57] Consequently, other superposition principles have been explored to study the dynamic mechanical response of homopolymers (*e.g.,* nylon) to variables other than temperature, such as: salt,[58, 59] pH,[40] and water/humidity.[60-62] In the specific case of the dynamic mechanical behavior of hydrated PECs, equivalent effects between time (frequency), temperature, salt, and pH have been proposed and studied for immersed PECs and/or PEC coacervates: time-temperature superposition,[37] time-salt superposition,[21, 24, 63] time-temperature-salt superposition,[37] and time-pH superposition.[40] Only two studies have addressed the application of the time-humidity superposition principle to PECs, however this was done for ion conductivity.[35, 39] Therefore, information is lacking regarding time-water-temperature superposition for the dynamic mechanical behavior of PECs.

Here, we study the plasticizing effects of water and temperature on the dynamic mechanical behavior of a PEC made from poly(allylamine hydrochloride) (PAH) and poly(acrylic acid) (PAA), as well as its mechanical behavior through the application of time-temperature (TTSP) and time-water (TWSP) superposition principles. PAH/PAA PEC specimens were equilibrated to specific relative humidity values and tested using a dynamic mechanical analysis (DMA)

instrument equipped with a relative humidity accessory. Data collected for the storage modulus (E') were used to construct master curves after the application of TTSP and TWSP from which two horizontal shift factors were assessed: a temperature-dependent shift factor (a_T) and a water-dependent shift factor (a_W). Finally, the temperature dependence of a_T and the water dependence of a_W were described using an Arrhenius equation and a log-linear equation, respectively. Such information is relevant to the selection of materials for specific applications in which the material's mechanical behavior under the conditions of use (*e.g.,* cyclic loading, temperature, relative humidity (water content), *etc*.) are important.

EXPERIMENTAL SECTION

Materials

Poly(acrylic acid) (PAA, Mw 100,000 g-mol^{-1}, 35 wt% aqueous solution) was purchased from Sigma Aldrich. Poly(allylamine hydrochloride) (PAH, Mw 120,000 – 200,000 g-mol^{-1}, 40 wt% aqueous solution) was purchased from Polysciences Inc. PAA and PAH were used as received. Milli-Q water was used for all experiments and solutions preparation.

Preparation of PAH/PAA Polyelectrolyte Complexes

A preparation procedure developed by Zhang *et al*.[38] was followed. 0.1 M solutions of PAH and PAA were prepared with respect to their repeat unit molar mass. The pH of the polyelectrolyte solutions was adjusted to pH 7 using NaOH or HCl aqueous solutions. 100 mL of the PAH solution were quickly added to 100 mL of the PAA solution. The PAH/PAA blend was stirred for 30 min at 600 rpm. Dialysis of the PAH/PAA PEC mixture was performed using Milli-Q water at pH 7 for 2 days. Dialysis time was determined by measuring the conductivity of the Milli-Q water. The dialyzed PEC was transferred to Falcon tubes and centrifuged for 10 min at 8500 rpm and 25 ºC. Centrifuged PECs were recovered, cut into small chunks, and allowed to dry at room conditions

for at least 12 hours. Once dry, the PEC chunks were ground into a powder. For improved reproducibility, multiple batches were prepared and then blended all together.

Solid specimens for dynamic mechanical testing and water content determination were prepared by compression molding according to ASTM D4703-16.[64] A stainless steel flash mold with machined cavities was used, having cavity dimensions of 20 mm length, 6 mm width, and 0.5 mm depth. 50 ± 1 mg of the powdered PAH/PAA PEC were carefully placed in each machined cavity. Then, 55 µl of Milli-Q water at pH 7 were added to each cavity. Aluminum foil 1100 was used as the separating sheet. The mold was placed in a hot press at 100 ^{o}F for a total of 14 minutes: 10 minutes without any load, 2 minutes with a 2 ton load, and 2 minutes with a 4 ton load. The PEC specimens were removed from the mold, placed between two glass slides to keep them flat, and allowed to dry for ~12 hours at ambient conditions.

Determination of PEC Water Content

Specimens were placed in a homebuilt humidity chamber at the desired RH value and room temperature. The mass of the hydrated PEC specimen was measured immediately after at least 24 hours of exposure in the RH chamber. The "dry" weight of the specimens was measured after drying the hydrated PEC specimens for 3 days in a vacuum oven at 30 ^{o}C. Longer exposure times in the humidity chamber did not increase the PEC water content. Therefore, a period of 24 hours was determined to be sufficient for the PEC specimens to reach the equilibrated water content (see **Table 1**).

Dynamic Mechanical Analysis Measurements

Mechanical testing was performed using a TA Q800 dynamic mechanical analyzer with a relative humidity accessory. A tension clamp configuration was used. PEC specimens were first equilibrated in the homebuilt humidity chamber for at least 24 hours at the desired RH value before

DMA measurements were taken. Multi-strain tests were performed to ensure all measurements were within the linear viscoelastic regime for each RH value (50, 70, 80, 85, 90 and 95% RH) (**Figure S1)**. A strain value of 0.01% was chosen for all multi-frequency strain tests.

Multi-frequency strain (frequency sweep) tests were performed at set temperature and relative humidity values over a 10^{-1} – 10^{1} Hz frequency range. PEC films were allowed to equilibrate for 30 – 40 min within the relative humidity accessory once the temperature and relative humidity set points were reached. Three frequency sweeps (~ 6 h) were performed to ensure an equilibrated response and to eliminate any mechanical history. Data from the third frequency sweep were used for time-temperature and time-water superposition analysis. Samples were tested in duplicates (except for 50% RH). A representative data set from each relative humidity-temperature configuration was chosen for plotting purposes. A new specimen was used for each relative humidity-temperature configuration.

Multi-frequency strain experiments provided information regarding the PEC mechanical behavior: storage (E') and loss (E") moduli as well as tan delta (E"/E'). A RH range of 50 – 95% was chosen due to sample and instrument limitations. Samples at 50% RH or less were glassy and brittle, thus often resulting in sample failure during experimental mounting. Therefore, RH values below 50% were not explored. The DMA relative humidity accessory presented limitations for RH and T ranges as well.[65] Upper and lower temperature limits were initially determined according to operating specifications for the DMA relative humidity accessory. Upper temperature limits were additionally narrowed down according to sample failure (yielding) at specific relative humidity values (see **Table 1**).

Table 1. Temperature ranges and increments used for frequency sweep tests and measured PEC water content (W_{H2O}) for different relative humidity values.

RH / %	W_{H2O} ± SD / wt%[a]	Measured Temperatures / °C
95*	35.7 ± N/A	25.0 - 40.0, ΔT = 2.5
90	31.7 ± 0.6	20.0 - 55.0, ΔT = 5.0
85	24.8 ± 0.4	20.0 - 55.0, ΔT = 5.0; 57.5
80	22.8 ± 0.5	20.0 - 65.0, ΔT = 5.0; 67.5
70	18.7 ± 0.8	20.0 – 80.0, ΔT = 10.0; 85.0, 90.0, 95.0
50	13.5 ± 0.8	20.0 - 90.0, ΔT = 10.0

[a] W_{H2O} was measured with a homebuilt humidity chamber at room temperature (~ 23 °C).

* Water content at 95% RH was estimated from the linear relationship between a_W and W_{H2O}.

Modulated Differential Scanning Calorimetry

Modulated DSC measurements were performed using a TA Q200 differential scanning calorimeter. A procedure developed by Shao and Lutkenhaus was followed to measure the glass transition temperature (T_g) of dry PAH and PAA polymers.[66] The T_g for hydrated PAH/PAA PECs was measured following a procedure developed by Zhang *et al.* (rate = 2 °C-min^{-1}, modulation period = 60 s, and modulation amplitude = ± 1.272 °C).[38] In this work, dried (3 d, 30 °C under vacuum) PEC powder was hydrated with Milli-Q water at pH 7. Sample masses ranged from 5 to 12 mg. Measurements were performed in duplicates for the dry polymers and in triplicates for the hydrated PECs.

Molecular Dynamics Simulations

The Gromacs 5.1.3 package[67, 68] was used for all-atom molecular dynamics (MD) simulations of assemblies consisting of 20 PAH_{20} and 20 PAA_{20} molecules. The subscript 20 refers to the

number of repeat units in each chain. The OPLS-aa force field[69] was used for polyelectrolytes and TIP4P explicit water model[70] for the water. The protonation of PAA and PAH was set so that all repeat units were fully charged, matching assembly at pH = 7.[71] The degrees of ionization of PAH and PAA within PAH/PAA assembled at pH 7 were estimated as 100% and 93%, respectively. Three different water concentrations, *i.e.*, 18.7, 24.8, and 31.7 wt%, corresponding to 70, 85, and 90% RH in the experiments, were examined. The chemical structures of PAA and PAH, and sample simulation snapshots of 20-mer PAH and PAA are presented in **Figure S2**.

The PME method[72] was used for the long-range electrostatics interactions and the Lennard-Jones potential with a 1.0 nm cut-off for the van der Waals interactions. Long-range dispersion corrections for energy and pressure were applied. The LINCS[73] and SETTLE[74] algorithms were used to constrain the bonds in the polyelectrolytes and in water molecules. A 2 fs time step within the leap-frog integration scheme was applied, and the trajectories were recorded every 1000 steps. Temperature was controlled via the V-rescale thermostat[75] with coupling constant $\tau = 0.1$ ps; the polyelectrolytes and solvent were coupled to separate heat baths. Periodic boundary conditions were applied in all directions. Pressure was maintained at 1 bar via the Parrinello-Rahman barostat[76] with coupling constant τ_p = 2 ps. The VMD software package was used for visualizations.[77] Initial PEC configurations were generated using PACKMOL[78] with a protocol established in previous work.[42, 79] Additional information about the simulation system preparation and analysis is provided in the Supporting Information.

RESULTS AND DISCUSSION

PEC water content and T_g

In order to understand the effect of water on the dynamic mechanical behavior of PAH/PAA PECs, their water content was determined at specific relative humidity (RH) values, **Figure 1** (see

Table S1 in Supporting Information for a sample calculation). A linear trend of water content with RH is observed between 50 and 85% RH. At 90% RH, the PEC absorbs more water from the environment due to increased rearrangement of the PEC structure with increasing RH.[80] This sudden increase in water content above 85% RH resembles a similar effect observed by Nolte *et al*.,[80] where polyelectrolyte multilayer (PEM) swelling significantly increased above 90% RH. **Figure S3** illustrates the glass transition temperature (T_g) as a function of water content in the PAH/PAA PEC. The T_g values measured for the PECs at varying RH values (water content) are in agreement with previously published T_g values for hydrated PAH/PAA PECs studied by Zhang *et al*.[38] T_g decreased with increasing water content, which is explained by the plasticizing effect of water.[81]

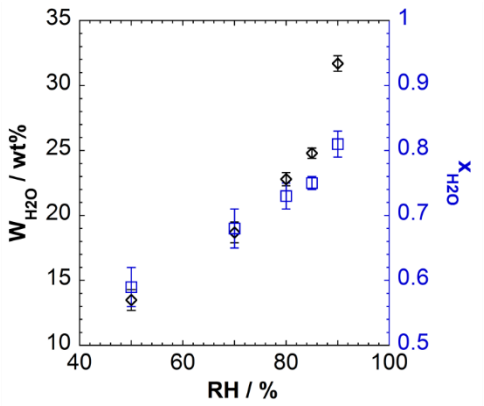

Figure 1. PAH/PAA PEC water content (◊, black) and water mole fraction (□, blue) as a function of relative humidity at 25 °C.

Time-Temperature Superpositioning Using Dynamic Mechanical Analysis

E' was measured over a 10^{-1} – 10^{1} Hz frequency range at different temperatures and relative humidity values (see **Table 1**). **Figure 2** presents the application of the time-temperature superposition principle (TTSP) for data taken at 90% RH. **Figure 2a** shows the behavior of E' at

different temperatures (20.0 – 55.0, ΔT = 5.0 ºC, where ΔT describes the temperature interval) as a function of frequency and where E' decreases with increasing temperature and decreasing frequency. This behavior can be attributed to weakening of the polymer-water hydrogen bonding network with increasing temperature, followed by polymer chain relaxation.[38] Notably, at higher temperatures and relative humidity the sample yielded due to heating through the glass transition. **Figure 2b** shows the master curve obtained after application of the TTSP with an arbitrarily chosen reference temperature (T_{ref}) of 40 ºC, where data in Figure 2a was shifted horizontally along the frequency axis using a temperature-dependent shift factor, $\mathbf{a_T}$.[56] Figure 2b shows a broader frequency range of 10^{-4} – 10^{6} Hz after the application of the TTSP to data taken in a 10^{-1} – 10^{1} Hz frequency range. Therefore, TTSP allows for the study of PAH/PAA PEC mechanical behavior over a frequency range beyond DMA capabilities (10^{-2} – 10^{2} Hz).

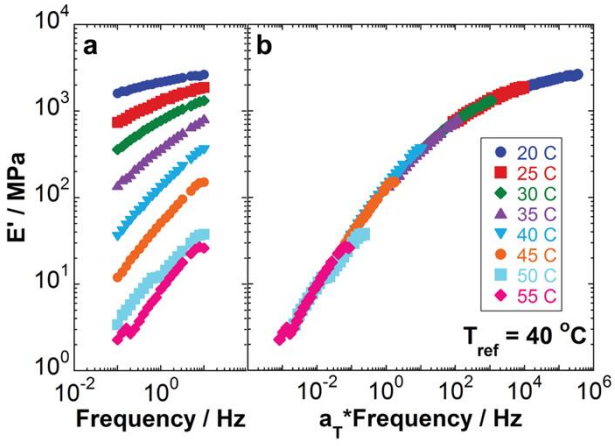

Figure 2. Application of the time-temperature superposition principle. a) E' data taken at 90% RH over a 10^{-1} – 10^{1} Hz frequency range and a 20.0 – 55.0 ºC temperature range. b) Time-temperature master curve made from experimental data in (a) with T_{ref} = 40 ºC. Legend in (b) applies to all panels. E' data taken over a 10^{-1} – 10^{1} Hz frequency range for 50 - 95% RH is shown in **Figure S4**. Tan delta data over the same frequency range, for all RH values, is presented in **Figure S5**.

Successful time-temperature superpositioning of data taken at different temperatures was obtained for RH values of 50, 70, 80, 85, 90, and 95%, indicating applicability of TTSP for PAH/PAA PECs. **Figure 3** shows the temperature dependence of a_T fitted using the Arrhenius equation (Equation 1), where E_a is the activation energy, R is the universal gas constant, T is temperature, and T_{ref} is the reference temperature. An attempt to fit a_T data using the WLF equation (Equation S1) was also made (see Supporting Information, **Figure S6** and **Table S2**). However, values for C_1 and C_2 (empirically adjustable parameters) were not reasonable for RH values below 90%. Additionally, the WLF equation should not be used for cases where: 1) $T > T_g + 100$ ºC, 2) $T < T_g$, and 3) the temperature range is small.[53] Therefore, the Arrhenius equation was deemed the best representation of the dynamic mechanical behavior of PAH/PAA PECs. This activation energy likely represents the activation barrier that must be overcome to break an intrinsic ion pair.

$$Ln(a_T) = \frac{E_a}{R}\left(\frac{1}{T} - \frac{1}{T_{ref}}\right)$$

Arrhenius equation (**Equation 1**)[56]

Superpositioning of the dynamic mechanical data may become ambiguous should the physical network structure change.[82] In other words, if the ratio of intrinsic to extrinsic ion pairs varies with strain, temperature, or humidity, then time-temperature and time-water superpositioning may be invalid. For example, Hu *et al*.[82] demonstrated such a case for time-temperature superpositioning for dual hydrogel networks containing reversible hydrogen bonds. Here in this work, to ensure that the physical network structure remained intact, a low strain value of 0.01% was used throughout the dynamic mechanical experiments (*e.g.,* see Figure S1). Additionally, to investigate the possibility of temperature or humidity effects on the physical network structure of the PEC, simulations were conducted and are discussed *vide infra*. From these simulations, we conclude that the fundamental nature of the physical PEC network does not change appreciably over the temperature and humidity ranges investigated.

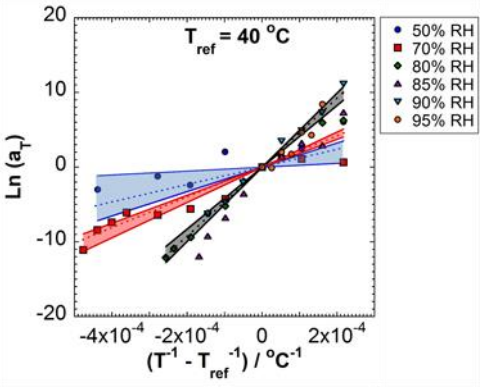

Figure 3. Temperature-dependent shift factors (a_T) for different relative humidity values (T_{ref} = 40 °C) and fits using the Arrhenius equation (dashed lines, Equation 1). 95% confidence intervals for the slope are represented by the shaded areas: 50% RH (blue), 70% RH (red), and 80 – 95% RH (black). The data sets for 80 – 95% RH are grouped and analyzed together because of their similar a_T trends.

The activation energy in the Arrhenius equation is related to small-scale molecular motions,[56] which here likely represent the dynamic relaxation of polyelectrolyte segments facilitated by the formation and reformation of polycation-polyanion intrinsic ion pairs. An activation energy of 379 ± 35 kJ-mol^{-1} (95% confidence interval) was calculated for RH values between 80 and 95%, which suggests that a_T is independent of relative humidity (water content) within that range. Figure 3 also shows activation energies of 176 ± 20 kJ-mol^{-1} and 78 ± 57 kJ-mol^{-1} for 70% RH and 50% RH, respectively. These results suggest that, although PAH/PAA PECs at lower humidities have higher storage moduli, the energy barriers for relaxation are lower. LaPlante and LeeSullivan discussed a similar observation using an Arrhenius relationship in hydrated epoxy samples, for which water could have dual stiffening/plasticization effects, depending on water content and the state of the absorbed water (singly hydrogen bonded *vs.* multiply hydrogen bonded).[83] **Table S3** in the

Supporting Information presents E_a values for other materials, where a wide range of E_a values is observed.

From examination of the trends in E', the glass transition temperature of the PEC was inferred. The T_g determined using DMA is usually obtained from a) a peak in the loss modulus (which "more closely denotes the initial drop of E' from the glassy state into the transition") or b) a peak in tan delta.[56] **Figure S7** presents E', E'', and tan delta data as a function of temperature for each RH value. No peaks in E'' or tan delta were observed, except for data taken at 90% RH where a peak in tan delta appeared at a temperature of 50 ºC. Therefore, T_g data was taken at the intersection of two tangents for E' and tan delta curves to capture the initial drop of E' (Figure S7), which in this work is referred as the onset T_g determined by DMA (onset $T_{g,\,DMA}$), **Table 2**. Onset T_g values of 80.0, 58.7, 40.0 and, < 20.0 ºC were observed for 70, 80, 85, and 90% RH values, respectively. In general, T_g values determined by MDSC ($T_{g,\,MDSC}$) are in agreement with onset T_g values determined by DMA (onset $T_{g,\,DMA}$).

Table 2. Comparison of T_g data obtained from MDSC and DMA measurements.

RH / %	W_{H2O} / wt% [a]	$T_{g,\,MDSC}$ / °C	Onset $T_{g,\,DMA}$ [b] / °C	Onset $T_{g,\,DMA}$ [c] / °C
95*	35.7 ± N/A	-[d]	-	-
90	31.7 ± 0.6	-[d]	-	< 20.0
85	24.8 ± 0.4	35.4 ± 0.4	34.8	40.0
80	22.8 ± 0.5	46.9 ± 0.7	55.8	58.7
70	18.7 ± 0.8	70.9 ± 0.3	72.2	80.0
50	13.5 ± 0.8	103.7 ± 0.6	-	-

[a] Water content calculated from exposure of PEC specimens to humidity in a homebuilt humidity chamber

[b] Onset T_g determined from tan delta in Figure S7.

[c] Onset T_g determined from E' in Figure S7, where a sharp decrease in E' occurs.

[d] T_g data for PEC specimens exposed to RH > 85% were not detected with MDSC.

* Water content at 95% RH was estimated from the linear relationship between a_W and W_{H2O}.

In reviewing the literature, only a few articles were found on the study of temperature effects on the dynamic mechanical behavior of PECs and on the application of the time temperature superposition principle.[37, 47, 84, 85] Shamoun,[37] Ali,[84] Wang,[47] and Sadman,[85] studied hydrated solid PECs and PEC coacervates, neglecting the effect of water content on the dynamic mechanical behavior of PECs. These studies, however, proved the successful application of the TTSP for PECs such as PDADMA/PSS (poly(diallyldimethylammonium chloride) / poly(styrene sulfonate)),[37, 84] PMMA/F127 (poly(methacrylic acid) / triblock copolymer Pluronic VR),[47] and PSS/QVP (poly(styrene sulfonate) / quaternized poly(4-vinylpyridine)).[85] In this work, the application of the TTSP was validated for PAH/PAA PECs. Most importantly, the effects of temperature on the

dynamic mechanical behavior of PECs were studied at different PEC hydration levels (13.5 – 35.7 wt%). Thus, providing novel information regarding the plasticizing effect of water when solid-liked PECs are partially hydrated, emulating real ambient conditions.

Time-Water Superpositioning Using Dynamic Mechanical Analysis

Using the time-temperature master curves for the six relative humidity values investigated (50, 70, 80, 85, 90, and 95%), a time-water superposition principle (TWSP) was applied. **Figure 4a** shows the set of time-temperature master curves in one single E' versus frequency plot, where E' decreases with increasing relative humidity (increasing water content). This behavior can be attributed to an increase in free volume with increasing water content and lubrication of the intrinsic ion pairs, which promotes structural rearrangement within the PEC.[25, 51] The time-temperature master curves were shifted horizontally along the frequency axis as TWSP was applied for an arbitrarily chosen reference relative humidity (RH_{ref}) of 80% (22.8 wt% H_2O), **Figure 4b.** Due to this additional data shifting, a second shift factor was defined here as the water-dependent shift factor, a_W. The time-water super master curve shown in Figure 4b corresponds to a doubly shifted hydrothermal master curve, which represents the time dependence of E' at a single reference temperature and a single reference relative humidity (water content). Therefore, the successful construction of the time-water super master curve indicates the applicability of the time-water superposition principle for PAH/PAA PECs. E', E'', and tan delta super master curves, with T_{ref} = 40 °C and RH_{ref} = 80%, are shown in **Figure S8a**. A relaxation time τ of about 10^8 sec was observed at a crossover frequency of $a_T a_w f = 10^{-8}$ Hz. This long relaxation time could correspond to the time required for a sufficient number of intrinsic ion pairs to rearrange, allowing for chain or segmental relaxation. The possible relevance of a vertical shift factor (*b*) was explored and deemed unnecessary, **Figure S8b**.

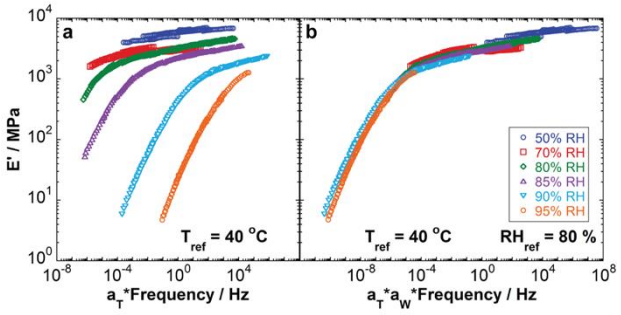

Figure 4. Application of the time-water superposition principle for PAH/PAA complexes. a) Time-temperature master curves for RH values of 50, 70, 80, 85, 90, and 95%. b) Time-water super master curve made from time-temperature master curves in (a) with RH_{ref} = 80% and T_{ref} = 40 ºC. Legend in (b) applies to all panels.

Analogous to TTSP, TWSP provides information regarding a water-dependent shift factor a_W. **Figure 5** shows the behavior of $\ln(a_W)$ as a function of different parameters. **Figure 5a** presents a non-linear behavior for $\ln(a_W)$ with RH, which is probably due to RH being related to the amount of water vapor present in the air — not to the amount of water present in the PEC. **Figures 5b-c** show a linear behavior for $\ln(a_W)$ as a function of water content (W_{H2O} / wt%) in the PEC, with Figure 5c taking into account the water content in the PEC at the RH_{ref}. Finally, **Figure 5d** shows a non-linear behavior for $\ln(a_W)$ as a function of partial vapor pressure (P_i), which was expected because P_i is directly related to the water vapor present in the air. An attempt to fit a_W data using a WLF-like equation (**Equation S2**) was also made (see Supporting Information, **Figure S9** and **Table S4**), but was not successful. Therefore, a log-linear equation (**Equation 2**), with a slope B and a y-intercept c, was proposed to fit a_W as a function of W_{H2O} instead of RH.

$$Ln(a_W) = B\left(W_{H2O} - W_{ref}\right) + c \qquad \textbf{(Equation 2)}$$

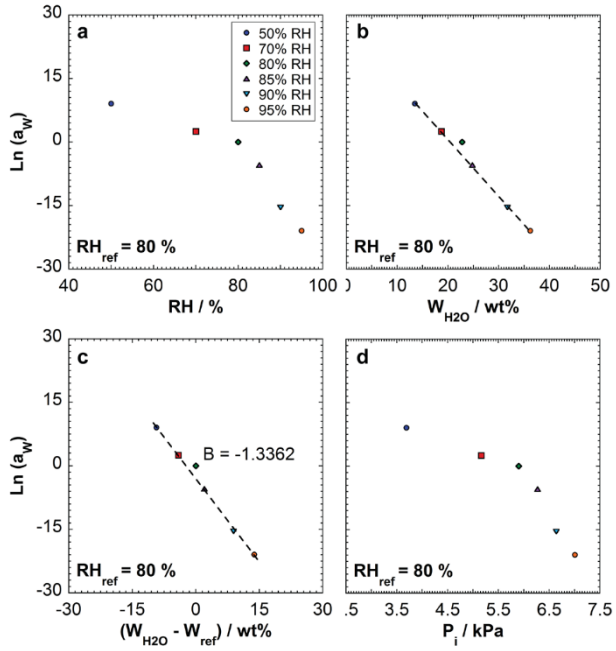

Figure 5. Water-dependent shift factor (a_W) as a function of: a) relative humidity; b) water content in the PEC ($\ln a_W = -1.34\ W_{H2O} + 27.9$, $R^2 = 0.9753$); c) water content in the PEC relative to a reference state ($\ln a_W = -1.34\ (W_{H2O} - W_{ref}) - 2.53$, $R^2 = 0.9870$); and d) partial vapor pressure. W_{ref}: W_{H2O} at the RH_{ref} (80% RH, 22.8 ± 0.5 wt%). RH_{ref} = 80% and T_{ref} = 40 ºC.

Effects of relative humidity (water content) on the dynamic mechanical behavior of PECs and the application of the TWSP to PECs or PEMs can be compared to recent work on time-humidity effects in PECs. De, Cramer, and Schönhoff studied the effect of relative humidity (or water content) on the ion conductivity of PECs and explored the application of a time-humidity superposition principle.[35, 39, 86] Most importantly, they proposed two equations: 1) a log-linear equation that captured the relationship between relative humidity and a humidity-dependent shift factor,[35] and 2) an equation that estimated the contribution of temperature to the humidity-dependent shift factor.[39] However, the latter was not explored over varying temperatures (see further explanation in Supporting Information).

In this work, the application of the TWSP provided a_W values that were fit using a log-linear equation (Equation 2) equivalent to the equation proposed by De *et al*.,[35] but applied here to the dynamic mechanical behavior of a PAH/PAA PEC as a function of water content instead of RH. Additionally, here we propose the shift factor a_c to describe the combined effects of TTSP and TWSP to our experimental data, **Equation 3**. E_a is the activation energy, R is the universal gas constant, T is temperature, T_{ref} is the reference temperature chosen during the application of the TTSP, B and c are the slope and the y-intercept of Equation 2, W_{H2O} is the water content in the PEC, and W_{ref} is the corresponding water content at the chosen reference relative humidity (RH_{ref}) during the application of the TWSP. Although Equation 3 appears similar to the equation proposed by Cramer *et al*.,[39] Equation 3 can actually be used to calculate a_c in order to predict a hydrothermal master curve. In this form, it becomes clear that B (which is determined experimentally to be negative in value) lowers the overall activation energy of the combined relaxation process with increasing water content.

$$a_c(T, W_{H2O}) = a_T a_W = exp\left[\frac{E_a}{R}\left(\frac{1}{T} - \frac{1}{T_{ref}}\right) + \left[B\left(W_{H2O} - W_{ref}\right) + c\right]\right] \quad \textbf{(Equation 3)}$$

As mentioned earlier, TTSP or TWSP may be inappropriate if the nature of the network exhibits large changes over the range of temperatures and humidities investigated. Here, our concern lies in quantifying whether the mobility of the network changes at the molecular level and whether the number of intrinsic ion pairs changes over the measurement. Because these factors are experimentally challenging to access in situ, we turn to molecular dynamics (MD) simulations of PAH/PAA PECs at corresponding water contents and temperatures. **Figure 6a** shows a representative snapshot of the PAH/PAA PEC in the simulations; the polyelectrolytes are entangled and their distribution, as well as water distribution, is relatively uniform. **Figure 6b** shows a set of mean square displacement (MSD) data sets for the PAH chains within the PECs in

simulations at different hydration and temperature conditions. Temperature and water content have very similar effects on the polyelectrolyte chain MSD; consequently, PAH chain mobility is similar for 70% RH at 55°C, 85% RH at 35°C, and 90% RH at 20°C. For a comparison, MSD for 70% RH at 20°C (blue line) and 90% RH at 55°C (green line) were also included. The same behavior was observed for PAA chains. The entire range of hydration and temperature MSD results both for PAA and PAH is provided in **Figure S10**.

Overall, increasing MSD with increasing hydration and temperature suggests an increase in the chain mobility. This is supported by a decrease in E' with both increasing hydration and increasing temperature as observed in the experimental DMA results. These findings provide an explanation for why these two factors can be superposed via the hydrogen bond network in the system presented in **Figure 6c** (*i.e.,* an intrinsic ion pair site with the closest water molecules around it and the formed hydrogen bond network). The similar responses of polyelectrolyte chain mobility to both variables, *i.e.,* hydration and temperature, could be related to the mobility of water molecules in PECs. For example, we have recently found that water mobility responds similarly for simulations of PDADMA/PSS complexes.[79]

The average number of intrinsic ion pairs formed by a single PAH repeat unit was calculated as a function of the temperature and water content, **Figure 6d**. The absolute number values of intrinsic ion pairs might differ slightly in simulations with different force-fields. However, as shown in reference [87] for ion-PE binding, the qualitative results can be expected to be insensitive of force-field. The changes in the number of intrinsic ion pairs within the studied temperature range are systematic, but relatively small in magnitude. For example, at T = 20 ^{o}C the average number of intrinsic ion pairs decreases slightly (from ~2.32 to ~2.00) with increasing hydration (from 70 to 90% RH). The calculated values for intrinsic ion pairs per PAH repeat unit at T = 20

°C equal 2.32 ± 0.02, 2.15 ± 0.05, and 2.00 ± 0.01 for 70, 85, and 90% RH, respectively. The decrease in the number of intrinsic ion pairs with increasing hydration might be explained by extra volume introduced by the added water molecules – polyelectrolytes are, on average, further apart. Notably, the intrinsic ion pair count exceeds one, as the polyelectrolytes form a complex 3D network. These simulation results suggest that TTSP is robust, as the number of intrinsic ion pairs does not change with temperatures. TWSP is also valid over this range because the number of intrinsic ion pairs changes only slightly.

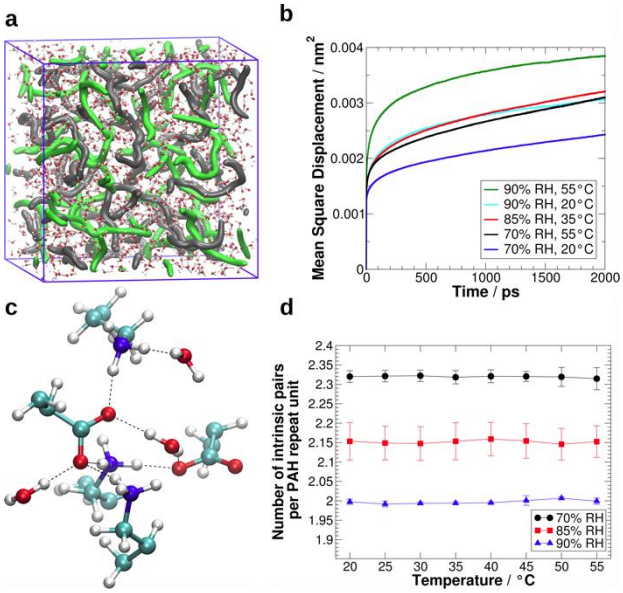

Figure 6. a) Representative snapshot of a PAH/PAA complex hydrated with 31.7 wt% water (90% RH) from MD simulations. PAA and PAH backbones are green and gray, respectively. The explicit water solvent is shown but polymer side chain chemistry is omitted in the visualization for clarity. b) Mean square displacement (MSD) of PAH chains at different hydration levels and temperatures. c) Snapshot showing an intrinsic ion pair in the simulations. Oxygen atoms are red, nitrogen atoms blue, and black dashed lines represent hydrogen bonds. d) Number of intrinsic ion pairs per single PAH repeat unit as a function of the temperature and relative humidity.

CONCLUSIONS

Application of superposition principles demonstrated equivalent effects of temperature and water on the dynamic mechanical behavior of PAH/PAA PECs. Temperature and water content strongly influenced the storage modulus, where E' decreased with both increasing temperature and increasing water content. The temperature-dependent shift factor (a_T) followed an Arrhenius relation, and the water-dependent shift factor (a_w) followed a log-linear relation with water content in the complex. Thus, the degree of plasticization in the PEC is controlled by its water content, which is determined by the relative humidity.[32] Consequently, the designation time-water superposition principle (TWSP) was deemed more appropriate than the previously used time-humidity superposition principle (THSP).

This led to the construction of a time–water super master curve (or hydrothermal master curve), and the proposal of a shift factor that combines the effect of water and temperature, a_c. Molecular simulations indicated the robustness of the application of TTSP and TWSP to the PEC, in that the mobility was similarly affected by temperature and water and that the number of intrinsic ion pairs did not change significantly. These results indicate that the rheological behavior of the PAH/PAA PECs is dominated by water and temperature. To place these findings in the context of our previous work, it may be suggested that water facilitates polymer relaxation by plasticization and lubrication at the intrinsic ion pair through a hydrogen bonding mechanism. Looking to the future, we plan to examine TWSP for other systems and conditions to further examine the significance of the B parameter from the log-linear a_w relation.

ASSOCIATED CONTENT

Supporting Information

The Supporting Information is available free of charge on the ACS Publications website. Supporting Information includes: strain sweeps, simulation system preparation and analysis, glass transition temperature of PAH/PAA PECs, loss modulus and tan delta data, a_T and a_W data fitting, and E_a values for other materials.

AUTHOR INFORMATION

Corresponding Author

E-mail address: jodie.lutkenhaus@tamu.edu

Present Addresses

[†]Jerzy Haber Institute of Catalysis and Surface Chemistry, Polish Academy of Sciences, Niezapominajek 8, PL-30239 Krakow, Poland

Author Contributions

The manuscript was written through contributions of all authors. All authors have given approval to the final version of the manuscript.

Funding Sources

This work was supported by the National Science Foundation (Grant No. 1609696) (J.L.L.) and Academy of Finland (Grant. No. 309324) (M.S.). This work was also supported by CSC – IT Center for Science, Finland, and RAMI – RawMatTERS Finland Infrastructure for computational resources.

Notes

The authors declare no competing financial interest.

ACKNOWLEDGMENT

This work was supported by the National Science Foundation (Grant No. 1609696) (J.L.L.) and Academy of Finland (Grant No. 309324) (M.S.). This work was also supported by CSC – IT Center for Science, Finland, and RAMI – RawMatTERS Finland Infrastructure for computational resources.

REFERENCES

1. Olek, M.; Ostrander, J.; Jurga, S.; Möhwald, H.; Kotov, N.; Kempa, K.; Giersig, M. Layer-by-Layer Assembled Composites from Multiwall Carbon Nanotubes with Different Morphologies. *Nano Letters* **2004,** 4 (10), 1889-1895 DOI: 10.1021/nl048950w.

2. Hyder, M. N.; Lee, S. W.; Cebeci, F. Ç.; Schmidt, D. J.; Shao-Horn, Y.; Hammond, P. T. Layer-by-Layer Assembled Polyaniline Nanofiber/Multiwall Carbon Nanotube Thin Film Electrodes for High-Power and High-Energy Storage Applications. *ACS Nano* **2011,** 5 (11), 8552-8561 DOI: 10.1021/nn2029617.

3. Fávero, V. O.; Oliveira, D. A.; Lutkenhaus, J. L.; Siqueira, J. R. Layer-by-layer nanostructured supercapacitor electrodes consisting of ZnO nanoparticles and multi-walled carbon nanotubes. *Journal of Materials Science* **2018,** 53 (9), 6719-6728 DOI: 10.1007/s10853-018-2010-4.

4. Cho, C.; Song, Y.; Allen, R.; Wallace, K. L.; Grunlan, J. C. Stretchable electrically conductive and high gas barrier nanocomposites. *Journal of Materials Chemistry C* **2018,** 6 (8), 2095-2104 DOI: 10.1039/C7TC05495E.

5. De, S.; Lutkenhaus, J. L. Corrosion behaviour of eco-friendly airbrushed reduced graphene oxide-poly(vinyl alcohol) coatings. *Green Chemistry* **2018,** 20 (2), 506-514 DOI: 10.1039/C7GC02882B.

6. Jeon, J.-W.; Kwon, S. R.; Lutkenhaus, J. L. Polyaniline nanofiber/electrochemically reduced graphene oxide layer-by-layer electrodes for electrochemical energy storage. *Journal of Materials Chemistry A* **2015,** 3 (7), 3757-3767 DOI: 10.1039/C4TA04697H.

7. Kwon, S. R.; Harris, J.; Zhou, T.; Loufakis, D.; Boyd, J. G.; Lutkenhaus, J. L. Mechanically Strong Graphene/Aramid Nanofiber Composite Electrodes for Structural Energy and Power. *ACS Nano* **2017,** 11 (7), 6682-6690 DOI: 10.1021/acsnano.7b00790.

8. Kwon, S. R.; Elinski, M. B.; Batteas, J. D.; Lutkenhaus, J. L. Robust and Flexible Aramid Nanofiber/Graphene Layer-by-Layer Electrodes. *ACS Applied Materials & Interfaces* **2017,** 9 (20), 17125-17135 DOI: 10.1021/acsami.7b03449.

9. Kwon, S. R.; Jeon, J.-W.; Lutkenhaus, J. L. Sprayable, paintable layer-by-layer polyaniline nanofiber/graphene electrodes. *RSC Advances* **2015,** 5 (20), 14994-15001 DOI: 10.1039/C4RA16822D.

10. Suarez-Martinez, P. C.; Robinson, J.; An, H.; Nahas, R. C.; Cinoman, D.; Lutkenhaus, J. L. Spray-On Polymer–Clay Multilayers as a Superior Anticorrosion Metal Pretreatment. *Macromolecular Materials and Engineering* **2017,** 302 (6), 1600552-n/a DOI: 10.1002/mame.201600552.

11. Suarez-Martinez, P. C.; Robinson, J.; An, H.; Nahas, R. C.; Cinoman, D.; Lutkenhaus, J. L. Polymer-clay nanocomposite coatings as efficient, environment-friendly surface pretreatments for aluminum alloy 2024-T3. *Electrochimica Acta* **2018,** 260, 73-81 DOI: https://doi.org/10.1016/j.electacta.2017.11.046.

12. Chakraborty, U.; Singha, T.; Chianelli, R. R.; Hansda, C.; Kumar Paul, P. Organic-inorganic hybrid layer-by-layer electrostatic self-assembled film of cationic dye Methylene Blue and a clay mineral: Spectroscopic and Atomic Force microscopic investigations. *Journal of Luminescence* **2017,** 187, 322-332 DOI: https://doi.org/10.1016/j.jlumin.2017.03.039.

13. Qiu, X.; Li, Z.; Li, X.; Zhang, Z. Flame retardant coatings prepared using layer by layer assembly: A review. *Chemical Engineering Journal* **2018,** 334, 108-122 DOI: https://doi.org/10.1016/j.cej.2017.09.194.

14. Rodrigues, J. R.; Alves, N. M.; Mano, J. F. Nacre-inspired nanocomposites produced using layer-by-layer assembly: Design strategies and biomedical applications. *Materials Science and Engineering: C* **2017,** 76, 1263-1273 DOI: https://doi.org/10.1016/j.msec.2017.02.043.

15. Holder, K. M.; Smith, R. J.; Grunlan, J. C. A review of flame retardant nanocoatings prepared using layer-by-layer assembly of polyelectrolytes. *Journal of Materials Science* **2017,** 52 (22), 12923-12959 DOI: 10.1007/s10853-017-1390-1.

16. Lutkenhaus, J. L.; Olivetti, E. A.; Verploegen, E. A.; Cord, B. M.; Sadoway, D. R.; Hammond, P. T. Anisotropic Structure and Transport in Self-Assembled Layered Polymer−Clay Nanocomposites. *Langmuir* **2007,** 23 (16), 8515-8521 DOI: 10.1021/la700432p.

17. Tsurko, E. S.; Feicht, P.; Nehm, F.; Ament, K.; Rosenfeldt, S.; Pietsch, I.; Roschmann, K.; Kalo, H.; Breu, J. Large Scale Self-Assembly of Smectic Nanocomposite Films by Doctor Blading versus Spray Coating: Impact of Crystal Quality on Barrier Properties. *Macromolecules* **2017,** 50 (11), 4344-4350 DOI: 10.1021/acs.macromol.7b00701.

18. O'Neal, J. T.; Bolen, M. J.; Dai, E. Y.; Lutkenhaus, J. L. Hydrogen-bonded polymer nanocomposites containing discrete layers of gold nanoparticles. *Journal of Colloid and Interface Science* **2017,** 485, 260-268 DOI: https://doi.org/10.1016/j.jcis.2016.09.044.

19. Fu, J.; Wang, Q.; Schlenoff, J. B. Extruded Superparamagnetic Saloplastic Polyelectrolyte Nanocomposites. *ACS Applied Materials & Interfaces* **2015,** 7 (1), 895-901 DOI: 10.1021/am5074694.

20. Eom, T.; Woo, K.; Cho, W.; Heo, J. E.; Jang, D.; Shin, J. I.; Martin, D. C.; Wie, J. J.; Shim, B. S. Nanoarchitecturing of Natural Melanin Nanospheres by Layer-by-Layer Assembly: Macroscale Anti-inflammatory Conductive Coatings with Optoelectronic Tunability. *Biomacromolecules* **2017,** 18 (6), 1908-1917 DOI: 10.1021/acs.biomac.7b00336.

21. Hamad, F. G.; Chen, Q.; Colby, R. H. Linear Viscoelasticity and Swelling of Polyelectrolyte Complex Coacervates. *Macromolecules* **2018,** 51 (15), 5547-5555 DOI: 10.1021/acs.macromol.8b00401.

22. Michaels, A. S.; Miekka, R. G. Polycation-polyanion complexes: Preparation and properties of Poly-(vinylbenzyltrimethylammonium) Poly-(styrenesulfonate). *The Journal of Physical Chemistry* **1961,** 65 (10), 1765-1773 DOI: 10.1021/j100827a020.

23. Porcel, C. H.; Schlenoff, J. B. Compact Polyelectrolyte Complexes: "Saloplastic" Candidates for Biomaterials. *Biomacromolecules* **2009,** 10 (11), 2968-2975 DOI: 10.1021/bm900373c.

24. Liu, Y.; Momani, B.; Winter, H. H.; Perry, S. L. Rheological characterization of liquid-to-solid transitions in bulk polyelectrolyte complexes. *Soft Matter* **2017**, DOI: 10.1039/C7SM01285C.

25. Schaaf, P.; Schlenoff, J. B. Saloplastics: Processing Compact Polyelectrolyte Complexes. *Advanced Materials* **2015,** 27 (15), 2420-2432 DOI: 10.1002/adma.201500176.

26. Meka, V. S.; Sing, M. K. G.; Pichika, M. R.; Nali, S. R.; Kolapalli, V. R. M.; Kesharwani, P. A comprehensive review on polyelectrolyte complexes. *Drug Discovery Today* **2017,** 22 (11), 1697-1706 DOI: https://doi.org/10.1016/j.drudis.2017.06.008.

27. Richardson, J. J.; Björnmalm, M.; Caruso, F. Technology-driven layer-by-layer assembly of nanofilms. *Science* **2015,** 348 (6233), DOI: 10.1126/science.aaa2491.

28. Mueller, R.; Köhler, K.; Weinkamer, R.; Sukhorukov, G.; Fery, A. Melting of PDADMAC/PSS Capsules Investigated with AFM Force Spectroscopy. *Macromolecules* **2005,** 38 (23), 9766-9771 DOI: 10.1021/ma0513057.

29. Jaber, J. A.; Schlenoff, J. B. Mechanical Properties of Reversibly Cross-Linked Ultrathin Polyelectrolyte Complexes. *Journal of the American Chemical Society* **2006,** 128 (9), 2940-2947 DOI: 10.1021/ja055892n.

30. Shamoun, R. F.; Reisch, A.; Schlenoff, J. B. Extruded Saloplastic Polyelectrolyte Complexes. *Advanced Functional Materials* **2012,** 22 (9), 1923-1931 DOI: 10.1002/adfm.201102787.

31. Nolte, A. J.; Rubner, M. F.; Cohen, R. E. Determining the Young's Modulus of Polyelectrolyte Multilayer Films via Stress-Induced Mechanical Buckling Instabilities. *Macromolecules* **2005,** 38 (13), 5367-5370 DOI: 10.1021/ma0507950.

32. Nolte, A. J.; Treat, N. D.; Cohen, R. E.; Rubner, M. F. Effect of Relative Humidity on the Young's Modulus of Polyelectrolyte Multilayer Films and Related Nonionic Polymers. *Macromolecules* **2008,** 41 (15), 5793-5798 DOI: 10.1021/ma800732j.

33. Hariri, H. H.; Lehaf, A. M.; Schlenoff, J. B. Mechanical Properties of Osmotically Stressed Polyelectrolyte Complexes and Multilayers: Water as a Plasticizer. *Macromolecules* **2012,** 45 (23), 9364-9372 DOI: 10.1021/ma302055m.

34. Toda, M.; Chen, Y.; Nett, S. K.; Itakura, A. N.; Gutmann, J.; Berger, R. Thin Polyelectrolyte Multilayers Made by Inkjet Printing and Their Characterization by Nanomechanical Cantilever Sensors. *The Journal of Physical Chemistry C* **2014,** 118 (15), 8071-8078 DOI: 10.1021/jp501464j.

35. De, S.; Cramer, C.; Schönhoff, M. Humidity Dependence of the Ionic Conductivity of Polyelectrolyte Complexes. *Macromolecules* **2011,** 44 (22), 8936-8943 DOI: 10.1021/ma201949s.

36. Lyu, X.; Clark, B.; Peterson, A. M. Thermal transitions in and structures of dried polyelectrolytes and polyelectrolyte complexes. *Journal of Polymer Science Part B: Polymer Physics* **2017,** 55 (8), 684-691 DOI: 10.1002/polb.24319.

37. Shamoun, R. F.; Hariri, H. H.; Ghostine, R. A.; Schlenoff, J. B. Thermal Transformations in Extruded Saloplastic Polyelectrolyte Complexes. *Macromolecules* **2012,** 45 (24), 9759-9767 DOI: 10.1021/ma302075p.

38. Zhang, Y.; Li, F.; Valenzuela, L. D.; Sammalkorpi, M.; Lutkenhaus, J. L. Effect of Water on the Thermal Transition Observed in Poly(allylamine hydrochloride)–Poly(acrylic acid) Complexes. *Macromolecules* **2016,** 49 (19), 7563-7570 DOI: 10.1021/acs.macromol.6b00742.

39. Cramer, C.; De, S.; Schönhoff, M. Time-Humidity-Superposition Principle in Electrical Conductivity Spectra of Ion-Conducting Polymers. *Physical Review Letters* **2011,** 107 (2), 028301.

40. Tekaat, M.; Butergerds, D.; Schonhoff, M.; Fery, A.; Cramer, C. Scaling properties of the shear modulus of polyelectrolyte complex coacervates: a time-pH superposition principle. *Physical Chemistry Chemical Physics* **2015,** 17 (35), 22552-22556 DOI: 10.1039/C5CP02940F.

41. Joshua T. O'Neal, K. G. W., Yanpu Zhang, Ian M. George, and Jodie L. Lutkenhaus. Comparison of KBr and NaCl effects on the glass transition temperature of hydrated layer-by-layer assemblies. *The Journal of Chemical Physics* **2018,** 149 (16), 163317 DOI: 10.1063/1.5037491.

42. Zhang, Y.; Batys, P.; O'Neal, J. T.; Li, F.; Sammalkorpi, M.; Lutkenhaus, J. L. Molecular Origin of the Glass Transition in Polyelectrolyte Assemblies. *ACS Central Science* **2018,** 4 (5), 638-644 DOI: 10.1021/acscentsci.8b00137.

43. Zhang, Q.; Smith, J. R.; Saraf, L. V.; Hua, F. Transparent humidity sensor using cross-linked polyelectrolyte membrane. *IEEE Sensors Journal* **2009,** 9 (7), 854-857 DOI: 10.1109/JSEN.2009.2024055.

44. Su, P.-G.; Cheng, K.-H. Layer-by-layer assembly of mica and polyelectrolyte for use in low-humidity sensor. *Sensors and Actuators B: Chemical* **2009,** 137 (2), 555-560 DOI: https://doi.org/10.1016/j.snb.2009.01.053.

45. Zhao, Q.; Lee, D. W.; Ahn, B. K.; Seo, S.; Kaufman, Y.; Israelachvili, Jacob N.; Waite, J. H. Underwater contact adhesion and microarchitecture in polyelectrolyte complexes actuated by solvent exchange. *Nature Materials* **2016,** 15, 407 DOI: 10.1038/nmat4539

https://www.nature.com/articles/nmat4539#supplementary-information.

46. Reisch, A.; Roger, E.; Phoeung, T.; Antheaume, C.; Orthlieb, C.; Boulmedais, F.; Lavalle, P.; Schlenoff, J. B.; Frisch, B.; Schaaf, P. On the Benefits of Rubbing Salt in the Cut: Self-Healing of Saloplastic PAA/PAH Compact Polyelectrolyte Complexes. *Advanced Materials* **2014,** 26 (16), 2547-2551 DOI: 10.1002/adma.201304991.

47. Wang, Y.; He, J.; Aktas, S.; Sukhishvili, S. A.; Kalyon, D. M. Rheological behavior and self-healing of hydrogen-bonded complexes of a triblock Pluronic® copolymer with a weak polyacid. *Journal of Rheology* **2017,** 61 (6), 1103-1119 DOI: 10.1122/1.4997591.

48. Zhang, H.; Wang, C.; Zhu, G.; Zacharia, N. S. Self-Healing of Bulk Polyelectrolyte Complex Material as a Function of pH and Salt. *ACS Applied Materials & Interfaces* **2016,** 8 (39), 26258-26265 DOI: 10.1021/acsami.6b06776.

49. Cuthbert, T. J.; Jadischke, J. J.; de Bruyn, J. R.; Ragogna, P. J.; Gillies, E. R. Self-Healing Polyphosphonium Ionic Networks. *Macromolecules* **2017,** 50 (14), 5253-5260 DOI: 10.1021/acs.macromol.7b00955.

50. Wang, C.; Duan, Y.; Zacharia, N. S.; Vogt, B. D. A family of mechanically adaptive supramolecular graphene oxide/poly(ethylenimine) hydrogels from aqueous assembly. *Soft Matter* **2017,** 13 (6), 1161-1170 DOI: 10.1039/C6SM02439D.

51. Zhang, R.; Zhang, Y.; Antila, H. S.; Lutkenhaus, J. L.; Sammalkorpi, M. Role of Salt and Water in the Plasticization of PDAC/PSS Polyelectrolyte Assemblies. *The Journal of Physical Chemistry B* **2017,** 121 (1), 322-333 DOI: 10.1021/acs.jpcb.6b12315.

52. Wang, Q.; Schlenoff, J. B. The Polyelectrolyte Complex/Coacervate Continuum. *Macromolecules* **2014,** 47 (9), 3108-3116 DOI: 10.1021/ma500500q.

53. Instruments, T., Dynamic Mechanical Analysis: Basic Theory & Applications Training. TA Instruments: pp 85, 92, 98, 210, 216 - 219.

54. Lutkenhaus, J. L.; Hrabak, K. D.; McEnnis, K.; Hammond, P. T. Elastomeric Flexible Free-Standing Hydrogen-Bonded Nanoscale Assemblies. *Journal of the American Chemical Society* **2005,** 127 (49), 17228-17234 DOI: 10.1021/ja053472s.

55. Reisch, A.; Tirado, P.; Roger, E.; Boulmedais, F.; Collin, D.; Voegel, J.-C.; Frisch, B.; Schaaf, P.; Schlenoff, J. B. Compact Saloplastic Poly(Acrylic Acid)/Poly(Allylamine) Complexes: Kinetic Control Over Composition, Microstructure, and Mechanical Properties. *Advanced Functional Materials* **2013,** 23 (6), 673-682 DOI: 10.1002/adfm.201201413.

56. Chartoff, R. P.; Menczel, J. D.; Dillman, S. H., Dynamic Mechanical Analysis (DMA). In *Thermal Analysis of Polymers*, John Wiley & Sons, Inc.: 2008; pp 401-409.

57. Van Gurp, M.; Palmen, J. Time-temperature superposition for polymeric blends. *Rheol. Bull* **1998,** 67 (1), 5-8.

58. Spruijt, E.; Cohen Stuart, M. A.; van der Gucht, J. Linear Viscoelasticity of Polyelectrolyte Complex Coacervates. *Macromolecules* **2013,** 46 (4), 1633-1641 DOI: 10.1021/ma301730n.

59. Spruijt, E.; Sprakel, J.; Lemmers, M.; Stuart, M. A. C.; van der Gucht, J. Relaxation Dynamics at Different Time Scales in Electrostatic Complexes: Time-Salt Superposition. *Physical Review Letters* **2010,** 105 (20), 208301.

60. Fabre, V.; Quandalle, G.; Billon, N.; Cantournet, S. Time-Temperature-Water Content equivalence on dynamic mechanical response of polyamide 6,6. *Polymer* **2018,** 137, 22 - 29 DOI: https://doi.org/10.1016/j.polymer.2017.10.067.

61. Ishisaka, A.; Kawagoe, M. Examination of the time–water content superposition on the dynamic viscoelasticity of moistened polyamide 6 and epoxy. *Journal of Applied Polymer Science* **2004,** 93 (2), 560-567 DOI: 10.1002/app.20465.

62. Zhou, S. M.; Tashiro, K.; Ii, T. Confirmation of universality of time–humidity superposition principle for various water-absorbable polymers through dynamic viscoelastic measurements under controlled conditions of relative humidity and temperature. *Journal of Polymer Science Part B: Polymer Physics* **2001,** 39 (14), 1638-1650 DOI: 10.1002/polb.1135.

63. Marciel, A. B.; Srivastava, S.; Tirrell, M. V. Structure and rheology of polyelectrolyte complex coacervates. *Soft Matter* **2018,** 14 (13), 2454-2464 DOI: 10.1039/C7SM02041D.

64. ASTM D4703-16 Standard Practice for Compression Molding Thermoplastic Materials into Test Specimens, Plaques, or Sheets. 2016.

65. Instruments, T. DMA-RH Accessory - Getting Started Guide. **2013**, 13.

66. Shao, L.; Lutkenhaus, J. L. Thermochemical properties of free-standing electrostatic layer-by-layer assemblies containing poly(allylamine hydrochloride) and poly(acrylic acid). *Soft Matter* **2010,** 6 (14), 3363-3369 DOI: 10.1039/C0SM00082E.

67. Lindahl, E.; Hess, B.; van der Spoel, D. GROMACS 3.0: a package for molecular simulation and trajectory analysis. *Molecular modeling annual* **2001,** 7 (8), 306-317 DOI: 10.1007/s008940100045.

68. Berendsen, H. J. C.; van der Spoel, D.; van Drunen, R. GROMACS: A message-passing parallel molecular dynamics implementation. *Computer Physics Communications* **1995,** 91 (1), 43-56 DOI: https://doi.org/10.1016/0010-4655(95)00042-E.

69. Jorgensen, W. L.; Tirado-Rives, J. The OPLS [optimized potentials for liquid simulations] potential functions for proteins, energy minimizations for crystals of cyclic peptides and crambin. *Journal of the American Chemical Society* **1988,** 110 (6), 1657-1666.

70. Jorgensen, W. L.; Madura, J. D. Temperature and size dependence for Monte Carlo simulations of TIP4P water. *Molecular Physics* **1985,** 56 (6), 1381-1392 DOI: 10.1080/00268978500103111.

71. Choi, J.; Rubner, M. F. Influence of the Degree of Ionization on Weak Polyelectrolyte Multilayer Assembly. *Macromolecules* **2005,** 38 (1), 116-124 DOI: 10.1021/ma048596o.

72. Essmann, U.; Perera, L.; Berkowitz, M. L.; Darden, T.; Lee, H.; Pedersen, L. G. A smooth particle mesh Ewald method. *The Journal of Chemical Physics* **1995,** 103 (19), 8577-8593 DOI: 10.1063/1.470117.

73. Hess, B.; Bekker, H.; Berendsen, H. J. C.; Fraaije, J. G. E. M. LINCS: A linear constraint solver for molecular simulations. *Journal of Computational Chemistry* **1997,** 18 (12), 1463-1472 DOI: doi:10.1002/(SICI)1096-987X(199709)18:12<1463::AID-JCC4>3.0.CO;2-H.

74. Miyamoto, S.; Kollman, P. A. Settle: An analytical version of the SHAKE and RATTLE algorithm for rigid water models. *Journal of Computational Chemistry* **1992,** 13 (8), 952-962 DOI: doi:10.1002/jcc.540130805.

75. Bussi, G.; Donadio, D.; Parrinello, M. Canonical sampling through velocity rescaling. *The Journal of Chemical Physics* **2007,** 126 (1), 014101 DOI: 10.1063/1.2408420.

76. Parrinello, M.; Rahman, A. Polymorphic transitions in single crystals: A new molecular dynamics method. *Journal of Applied Physics* **1981,** 52 (12), 7182-7190 DOI: 10.1063/1.328693.

77. Humphrey, W.; Dalke, A.; Schulten, K. VMD: Visual molecular dynamics. *Journal of Molecular Graphics* **1996,** 14 (1), 33-38 DOI: https://doi.org/10.1016/0263-7855(96)00018-5.

78. Martínez, L.; Andrade, R.; Birgin, E. G.; Martínez, J. M. PACKMOL: A package for building initial configurations for molecular dynamics simulations. *Journal of Computational Chemistry* **2009,** 30 (13), 2157-2164 DOI: 10.1002/jcc.21224.

79. Batys, P.; Zhang, Y.; Lutkenhaus, J. L.; Sammalkorpi, M. Hydration and Temperature Response of Water Mobility in Poly(diallyldimethylammonium)–Poly(sodium 4-styrenesulfonate) Complexes. *Macromolecules* **2018,** 51 (20), 8268-8277 DOI: 10.1021/acs.macromol.8b01441.

80. Secrist, K. E.; Nolte, A. J. Humidity Swelling/Deswelling Hysteresis in a Polyelectrolyte Multilayer Film. *Macromolecules* **2011,** 44 (8), 2859-2865 DOI: 10.1021/ma101983s.

81. Fujita, H.; Kishimoto, A. Diffusion-controlled stress relaxation in polymers. II. Stress relaxation in swollen polymers. *Journal of Polymer Science* **1958,** 28 (118), 547-567 DOI: 10.1002/pol.1958.1202811806.

82. Hu, X.; Zhou, J.; Daniel, W. F. M.; Vatankhah-Varnoosfaderani, M.; Dobrynin, A. V.; Sheiko, S. S. Dynamics of Dual Networks: Strain Rate and Temperature Effects in Hydrogels

with Reversible H-Bonds. *Macromolecules* **2017,** 50 (2), 652-659 DOI: 10.1021/acs.macromol.6b02422.

83. Gabriel, L.; Pearl, L.-S. Moisture effects on FM300 structural film adhesive: Stress relaxation, fracture toughness, and dynamic mechanical analysis. *Journal of Applied Polymer Science* **2005,** 95 (5), 1285-1294 DOI: doi:10.1002/app.21353.

84. Ali, S.; Prabhu, V. Relaxation Behavior by Time-Salt and Time-Temperature Superpositions of Polyelectrolyte Complexes from Coacervate to Precipitate. *Gels* **2018,** 4 (1), 11.

85. Sadman, K.; Wang, Q.; Chen, Y.; Keshavarz, B.; Jiang, Z.; Shull, K. R. Influence of Hydrophobicity on Polyelectrolyte Complexation. *Macromolecules* **2017,** 50 (23), 9417-9426 DOI: 10.1021/acs.macromol.7b02031.

86. De, S.; Ostendorf, A.; Schönhoff, M.; Cramer, C. Ion Conduction and Its Activation in Hydrated Solid Polyelectrolyte Complexes. *Polymers* **2017,** 9 (11), DOI: 10.3390/polym9110550.

87. Batys, P.; Luukkonen, S.; Sammalkorpi, M. Ability of the Poisson–Boltzmann equation to capture molecular dynamics predicted ion distribution around polyelectrolytes. *Physical Chemistry Chemical Physics* **2017,** 19 (36), 24583-24593 DOI: 10.1039/C7CP02547E.

For Table of Contents use only

Time-Temperature and Time-Water Superposition Principles Applied to Poly(allylamine) / Poly(acrylic acid) Complexes

Pilar C. Suarez-Martinez[a], Piotr Batys[b,c,†], Maria Sammalkorpi[b] and Jodie L. Lutkenhaus[a,]*